

Functional Analysis of the Structural Basis of Homophilic Cadherin Adhesion

B. Zhu,* S. Chappuis-Flament,[†] E. Wong,[‡] I. E. Jensen,[§] B. M. Gumbiner,[¶] and D. Leckband*[§]

*Department of Chemical and Biomolecular Engineering, University of Illinois, Urbana, Illinois 61801 USA; [†]TRANSAT, Faculté de Médecine, 69373 Lyon Cedex 08, France; [‡]Department of Cell Biology, Rockefeller University, New York, New York 10021 USA; [§]Department of Biochemistry, University of Illinois, Urbana, Illinois 61801 USA; and [¶]Department of Cell Biology, University of Virginia School of Medicine, Charlottesville, Virginia 22908 USA

ABSTRACT The structures of many cell surface adhesion proteins comprise multiple tandem repeats of structurally similar domains. In many cases, the functional significance of this architecture is unknown, and there are several cases in which evidence for individual domain involvement in adhesion has been contradictory. In particular, the extracellular region of the adhesion glycoprotein cadherin consists of five tandemly arranged domains. One proposed mechanism postulated that adhesion involves only *trans* interactions between the outermost domains. However, subsequent investigations have generated several competing models. Here we describe direct measurements of the distance-dependent interaction potentials between cadherin mutants lacking different domains. By quantifying both the absolute distances at which opposed cadherin fragments bind and the quantized changes in the interaction potentials that result from deletions of individual domains, we demonstrate that two domains participate in homophilic cadherin binding. This finding contrasts with the current view that cadherins bind via a single, unique site on the protein surface. The potentials that result from interactions involving multiple domains generate a novel, modular binding mechanism in which opposed cadherin ectodomains can adhere in any of three antiparallel alignments.

INTRODUCTION

The structures of many adhesion proteins comprise multiple tandem repeats of similar domains (Chothia and Jones, 1997; Walsh and Doherty, 1997). The functional roles of these architectures is often unknown, and attempts to identify the functional domains have often yielded contradictory results (Ranheim et al., 1996; Kiselyov et al., 1997; Jensen et al., 1999). These large structures could play a scaffolding role, presenting the binding domains to receptors on opposing cells or maintaining intermembrane separations (Davis and van der Merwe, 1996). Flexibly-tethered receptors could also influence adhesion dynamics (Wong et al., 1997). A fundamental understanding of the structural basis of the adhesive function of these molecules is critical for understanding how they mediate a myriad of critical intercellular interactions. However, determining how these structures influence function requires quantifying both the adhesion and the range of protein interactions.

The extracellular segments of the classical cadherins comprise five tandem repeats of homologous, cadherin-type extracellular (EC) domains, EC1-5, which are numbered from the outermost N-terminal domain (Takeichi, 1991; Yap et al., 1997b). Cadherins are essential cell surface glycoproteins, and they mediate adhesion between adjacent cells in all soft tissues (Takeichi, 1995; Gumbiner, 1996). Early

studies suggested that the tissue selectivity function resides in the N-terminal EC domain, EC1 (Nose et al., 1990).

Several biophysical and structural studies attempted to identify the molecular basis of cadherin adhesion. Focusing on the N-terminal domains, investigations probed the possible mechanisms by which the proteins form both lateral dimers and *trans* adhesive bonds. Cadherin forms lateral dimers, which appear to be required for *trans* adhesion (Brieher et al., 1996; Yap et al., 1997a, 1998). The first published structure of the EC1 domain suggested that lateral dimerization involves inserting Trp-2 from one cadherin into a hydrophobic pocket on the adjacent protein (Shapiro et al., 1995). Some studies supported the Trp-2-dependent *cis* dimerization model (Shan et al., 2000; Klingelhöfer et al., 2002), but others suggested that *cis* dimerization is Trp-2-independent (Ahrens et al., 2002). In other structures, Trp-2 was free or even bound to the hydrophobic pocket on the same molecule (Koch et al., 1999; Pertz et al., 1999). Recent NMR studies of EC12 revealed that lateral dimerization perturbs residues near Trp-2, but did not confirm its direct involvement (Häussinger et al., 2002).

Several different adhesive interfaces have also been proposed based on multiple crystal structures of EC1 and EC12 fragments from both neural (N) and epithelial (E) cadherins (Nagar et al., 1995; Tomschy et al., 1996; Tamura et al., 1998; Koch et al., 1999; Pertz et al., 1999; Leckband and Sivasankar, 2000). The initially proposed adhesive interface involved a 3000 Å² region between opposed N-terminal (EC1) domains (Shapiro et al., 1995), but mutagenesis studies disproved this (Boggon et al., 2002). A recent structure of the full-length cadherin extracellular domain suggested yet a different adhesive contact (Boggon

Submitted October 1, 2002, and accepted for publication February 7, 2003.

Address reprint requests to D. Leckband, Dept. of Chemical and Biomolecular Engineering, University of Illinois, 600 S. Mathews Ave., Urbana, IL 61801. Tel.: 217-244-0793; Fax: 217-333-5052; E-mail: leckband@uiuc.edu.

© 2003 by the Biophysical Society

0006-3495/03/06/4033/10 \$2.00

et al., 2002). In this model, a putative *trans* adhesive bond forms by inserting Trp-2 from one N-terminal domain into the hydrophobic pocket on the N-terminal domain of an opposed protein (Boggon et al., 2002). Although the W2A substitution has been shown to abolish adhesion (Ahrens et al., 2002), this model differs from all others proposed previously (Tomschy et al., 1996; Tamura et al., 1998; Koch et al., 1999; Pertz et al., 1999; Leckband, 2002). Moreover, the NMR study of EEC12 showed that *cis* dimerization involved a large region near the Trp-2 site, but the Trp-2 residue is mobile in all of the aggregate forms observed (Häussinger et al., 2002). The oligomers also exhibited different symmetry than in the crystal lattice (Häussinger et al., 2002).

The investigations described above all focused exclusively on the interactions of the N-terminal domains. Despite their differences, models proposing that cadherins bind solely through their N-terminal domains predict that the proteins adhere at an intermembrane distance of 400–450 Å (Shapiro et al., 1995) or, if the proteins are rigidly bent, at 385 Å (Boggon et al., 2002). This hypothesis was directly tested, by measuring the distance-dependence of the interaction energy between oriented cadherin monolayers (Sivasankar et al., 1999, 2001). A distinct advantage of the force measurements is that they quantify both the force and the absolute distance, within ± 1 Å, between two surfaces (Israelachvili, 1973). The normalized forces were thus measured between oriented cadherin monolayers as a function of their separation, and hence of the relative cadherin alignments. The surprising result was that cadherins did not bind at the single intermembrane distance predicted by the models described above. Instead, the proteins bound at three different surface separations, which each corresponded to different, antiparallel alignments of the opposing proteins (Sivasankar et al., 1999, 2001). In contrast to the predicted behavior, the results demonstrated that homophilic cadherin adhesion involves domains in addition to EC1 (Sivasankar et al., 2001). A separate atomic force microscopy study of homophilic binding between E-cadherin extracellular domains also exhibited three different populations of bond strengths (Baumgartner et al., 2000).

Other studies support the hypothesis that multiple cadherin domains participate in homophilic adhesion. Flow assay investigations of cell adhesion to cadherin mutants lacking different regions of the extracellular segment confirmed that potent adhesion requires more than EC1, and strong adhesion requires at least EC1-3 (Chappuis-Flament et al., 2001). Those findings suggested that EC3 might also be somehow involved in binding. A different study showed that the deletion of the outer N-terminal domain of epithelial cadherin (EEC1) did not abolish adhesion (Renaud-Young and Gallin, 2002). Although cells expressing E-cadherin fragments lacking EC1 did not aggregate, they did adhere to cells expressing the full-length extracellular domain. Additionally, in contrast to previous

studies suggesting that mutations of the conserved HAV sequence in the N-terminal domain would abolish adhesion, permutations of the HAV sequence did not impair E-cadherin-mediated cell aggregation (Renaud-Young and Gallin, 2002).

The functional domains responsible for the observed behavior in the cell adhesion, bead aggregation, or force measurements could not be determined by those measurements alone. Although cell adhesion assays quantify relative adhesion strengths and bead aggregation measurements assess relative protein affinities, neither measurement can directly elucidate the molecular basis of the observed behavior. When protein binding involves single, well-defined binding sites, the interpretation of a single measured parameter is relatively straightforward. However, in cases involving multiple binding interactions, neither of these approaches can directly observe the interplay of different structural modules and their impact on the binding measurement. The latter is also true of crystal structures, which reflect only one of the possible interactions, and which are also frequently influenced by crystal packing forces. On the other hand, although surface force measurements do probe the molecular level interactions, the one-dimensional force profiles alone cannot identify the protein fragments mediating the adhesive behavior (Sivasankar et al., 2001).

This report describes direct measurements of the distance dependence of interactions between cadherin domain deletion mutants. These measurements demonstrated directly that this modular ectodomain architecture supports multiple, adhesive interactions, and identified the domains responsible for this behavior. These studies were carried out with different fragments of the C-cadherin ectodomain from *Xenopus* (FcCEC1-5) (Chappuis-Flament et al., 2001). Five cadherin deletion mutants were used to dissect the individual domains mediating homophilic adhesion (Table 1). These mutants were characterized previously in cell adhesion and bead aggregation assays (Chappuis-Flament et al., 2001). The ability to quantify the absolute surface separations within ± 1 Å allowed us to distinguish between different relative alignments of adhering cadherin fragments (Israelachvili, 1973). The resulting quantized shifts in the potentials after the deletion of single domains, and the effects of domain deletions on each of the three adhesive alignments, demonstrated the participation of both EC1 and EC3 in binding. The interaction of multiple domains generates a novel, modular

TABLE 1 Protein surface coverage measured by SPR

Cadherin construct	Surface coverage (protein/ μm^2)
FcCEC1-5	$9.9 \pm 0.4 \times 10^3$
FcCEC1-4	$1.2 \pm 0.4 \times 10^4$
FcCEC1-3	$1.4 \pm 0.4 \times 10^4$
FcCEC1-2	$1.7 \pm 0.4 \times 10^4$
FcCEC1245	$1.1 \pm 0.4 \times 10^4$
FcCEC345	$1.2 \pm 0.4 \times 10^4$

adhesion mechanism in which opposing cadherin ectodomains can adhere in any of three antiparallel alignments.

EXPERIMENTAL PROCEDURES

Materials

The lipids di-palmitoyl-phosphatidyl-ethanolamine (DPPE) and di-tritanyol-phosphatidylcholine (DTPC) were from Avanti Polar Lipids (Alabaster, AL). Nitrilo-triacetic acid-modified dilauryl glycerol ester (NTA-DLGE) was custom synthesized by Northern Lipids (Vancouver, BC). Tris buffer was purchased from Sigma, (St. Louis, MO) and all high purity salts were from Aldrich (St. Louis, MO).

Cadherin constructs were purified from cultures of stably transfected Chinese hamster ovary (CHO) cells according to published procedures (Chappuis-Flament et al., 2001). A dimer of the B domain of protein A fused to a C-terminal hexahistidine tag (SpA_{B2}) was overexpressed in *E. coli*, and isolated from cells according to published procedures (Johnson, C., I. Jensen, A. Prakasam, R. Vijayendran, and D. Leckband, unpublished results).

Protein monolayers

The Fc-cadherin constructs, purified as described previously (Chappuis-Flament et al., 2001), were immobilized to oriented hexahistidine-tagged B domains of protein A (SpA_{B2}). The protein A was bound to planar membranes containing lipids with nitrilo-triacetic acid (NTA)-modified headgroups (Fig. 1) (Sivasankar et al., 2001). The planar bilayers were prepared by Langmuir-Blodgett deposition and were supported on freshly cleaved, atomically flat mica surfaces. The first lipid monolayer consisted of gel phase DPPE that was deposited onto the mica sheets from the air-water interface at a density of 43 Å²/lipid (Fig. 1). The outermost lipid monolayer, which was in contact with the solution, contained 75 mol% NTA-DLGE and 25 mol% DTPC. The latter lipid monolayer was deposited onto the DPPE film from a subphase containing 10 mM Tris buffer, 150 mM NaNO₃, 25 μM NiSO₄, and 2 mM CaCl₂ at pH 7 and 25°C. The average lipid density was 65 Å²/lipid (Fig. 1). The melting temperature of DTPC is 4°C, so the outer lipid monolayers are fluid at the experimental temperature of 25°C. Fluorescence imaging confirmed that the two lipid components were well-mixed and homogeneously distributed. Additionally, proteins bound to these monolayers were similarly homogeneously distributed.

SpA_{B2} was immobilized on the bilayers by adsorption from a 1 μM protein solution containing 10 mM Tris buffer, 150 mM NaNO₃, 25 μM NiSO₄, and 2 mM CaCl₂ at pH 7.0. After the adsorption, the protein

monolayer was rinsed with buffer lacking protein. The Fc-cadherin was then bound to the SpA_{B2} monolayer by incubating the latter with a 0.3–0.5 μM cadherin solution. After a 3-h adsorption at room temperature, the protein monolayer was rinsed with pure buffer. The Fc-cadherin constructs bound to the immobilized SpA_{B2} with nanomolar affinity.

The assembly of the cadherin monolayers was monitored using a home-built surface plasmon resonance (SPR) instrument (Lavrik and Leckband, 2000) based on the Kretschmann configuration. A Teflon flow cell housing the NTA-DLGE monolayer was attached to a sample stage, which was rotated by a precision goniometer driven by a stepper motor. A Si photodiode detector monitored the intensity of a GaAs laser beam reflected off the gold film as a function of the external angle of incidence. Shifts in the resonance angle, at which the reflected light intensity is a minimum, were monitored continuously during protein adsorption to the lipid film. These shifts were then converted to changes in the effective optical thickness of the adsorbed protein monolayer by fitting the resonance curves to the Fresnel equations for a multilayer film. We then estimated the amount of bound protein from changes in the index of refraction of the adsorbed layer (Sivasankar et al., 2001). To do this, we assumed a 270 Å cadherin monolayer thickness for the full-length protein. This includes the 45 Å Fc domain plus the 225 Å ectodomain (Pokutta et al., 1994; Sivasankar et al., 2001; Boggon et al., 2002; Martel et al., 2002). An appropriately reduced thickness was used for each of the cadherin fragments. We used a refractive index of 1.45 for the pure protein.

For the SPR measurements, the NTA-lipid monolayers, at the same lipid density and composition as used in the force measurements, were deposited onto a hexadecanethiol monolayer. The latter monolayer was self-assembled on the evaporated gold film from a 1 mM ethanolic solution at room temperature (Sivasankar et al., 2001).

Force measurements

The interaction potentials between oriented monolayers of cadherin extracellular domains were measured with a Mark II surface force apparatus (SFA). This instrument quantifies the net force between two surfaces as a function of the absolute surface separation D , both during approach and separation (Israelachvili, 1992a,b). In these investigations, the proteins are supported on the surfaces of two crossed-cylindrical disks milled to a 2-cm radius R . When the radii are much greater than the range of the force, $R \gg D$, then the total integrated force between the materials on these macroscopic surfaces, e.g., proteins, is proportional to the interaction energy per unit area between two equivalent flat surfaces—that is, $F_c/R = 2\pi E$ (Israelachvili, 1973, 1992a,b; Israelachvili and Adams, 1978; Sivasankar et al., 2001). This is the well-established Derjaguin approximation, which is derived in several textbooks (Hunter, 1989; Israelachvili, 1992b). Thus, from measurements of the normalized force between two surfaces, the SFA quantifies the interaction potential between the materials (Israelachvili, 1992a; Wong et al., 1997; Sivasankar et al., 2001).

The adhesion energy density E_{ad} is determined from the force required to separate the surfaces, or the pull-off force F_{po} , and the Johnson-Kendall-Roberts (JKR) theory for the adhesion between deformable, curved surfaces (Johnson et al., 1971; Israelachvili, 1992b). The JKR theory states that F_{po} and the adhesion energy per area E_{ad} are related by $F_{po}/R = 1.5 \pi E_{ad}$ (Johnson et al., 1971; Israelachvili, 1992b). In these measurements, F_{po} is the maximal attractive force measured at the point of adhesive failure and abrupt surface separation. Importantly, under near-equilibrium pulling conditions when the rate of loading is much slower than the intrinsic dissociation rate of the bonds, F_{po} is determined by the maximum maximum gradient in the intersurface potential (Leckband and Israelachvili, 2001). The slow loading rates of typical SFA measurements, in which pull-off occurs over several seconds to minutes, approach near-equilibrium loading conditions. In this study, this was confirmed by the rate-independence, within the limits of error, of the measured adhesion energies. That is, the adhesion was the same whether the proteins were separated in 30 s or in 30 min.

The adhesion energy per bond is estimated by normalizing the adhesion energy per area by the average cadherin density on the membranes. Some

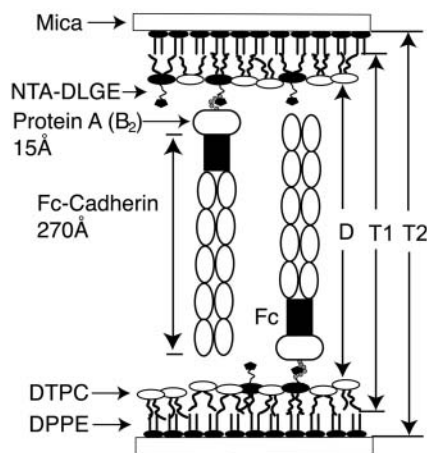


FIGURE 1 Schematic of the cadherin monolayers used in this study.

bond convection to the perimeter of the contact area could occur during membrane detachment (Vijayendran et al., 1998). The bond accumulation on the time frame of the measurement should be relatively low due to the high densities and slow diffusion coefficients of the immobilized proteins. Nevertheless, the convection will be similar for all of the cadherin fragments studied and will not influence the relative differences in the measured adhesion.

The force measurements were carried out with the samples bathed in 10 mM Tris buffer, containing 150 mM NaNO₃, 25 μM NiSO₄, and 2 mM CaCl₂ at pH 7.0. The temperature was maintained at 25 ± 1°C.

Definition of $D = 0$

In measurements of the normalized force versus the separation distance between identical cadherin monolayers, the distance D is the separation between the surfaces of the supporting lipid bilayers (Fig. 1). The interferometric technique of the SFA enables the absolute distance to be measured in situ within ±1 Å (Israelachvili, 1973). The interbilayer distance D was determined in two ways. In the first approach, we determined the change in total thickness T_1 (Fig. 1) of the molecular assembly between the crystalline DPPE monolayers after depositing the NTA-DLGE/DTPC monolayer and immobilizing the proteins. Thus $D = T_1 - 2 \times T_{\text{NTA-DLGE}}$ where $T_{\text{NTA-DLGE}}$ is the thickness of the NTA-DLGE monolayer. The cadherin and SpA_{B2} thickness was then determined from the distance D at the onset of the repulsive force between the protein and a bare lipid or between two dilute cadherin monolayers. In the second approach, the thickness of the organic layers between the mica substrates T_2 (Fig. 1) was determined. After draining the apparatus of buffer solution, the surfaces were rinsed with deionized water and all organic layers were removed by UV irradiation. Thus, the membrane-membrane separation $D = T_2 - 2 \times (T_{\text{DPPE}} + T_{\text{NTA-DLGE}})$, where T_{DPPE} is the thickness of the DPPE monolayer. The 27 Å thickness of a DPPE film was reported previously (Marra and Israelachvili, 1985; Sivasankar et al., 1999), and the 32 Å thickness of the NTA-DLGE monolayer was determined by x-ray reflectivity (Martel et al., 2002). The NTA headgroup dimensions are 15 ± 1 Å (Martel et al., 2002). Thus, because the bilayer thickness is determined independently and either T_1 or T_2 is measured directly in every experiment, $D = 0$, and hence the intersurface distance is determined unambiguously. This differs from other force probe techniques, which only measure relative changes in separation but not the absolute distance between the materials (Leckband and Israelachvili, 2001).

Identifying multiple adhesive interactions between cadherin ectodomains

With the cadherin monolayers, the measured interbilayer distance allows the determination of both the thickness of the cadherin monolayers and their extent of interdigitation. This accuracy in the absolute distance measurements allows the precise control of the intersurface separation, and hence the relative overlap between opposed cadherin monolayers. To measure adhesion between the cadherins in different relative alignments, the intersurface distance D was decreased to some value between 330 Å, corresponding to full overlap between FcCEC1-5 proteins, for example, and 600 Å, which would correspond to slight contact between the outer domains only. Upon separating the surfaces from the different overlap distances, we then measured the position at which the maximal attraction developed between the proteins. If the proteins bound at a single site, then adhesion occurred at a unique distance. Multiple binding interactions generate adhesion at multiple distances (Sivasankar et al., 1999, 2001). This approach has been used in numerous investigations with the surface force apparatus to measure oscillatory intersurface potentials that display multiple attractive minima, which occur at different surface separations (Israelachvili and Pashley, 1983; Christenson et al., 1987; Israelachvili, 1987; Kekicheff et al., 1990; Leckband et al., 1995; Petrov et al., 1995).

RESULTS AND DISCUSSION

The cadherin surface densities were quantified by SPR as described previously (Sivasankar et al., 2001). In these measurements, upon protein injection into the flow cell, subsequent protein adsorption causes a change in the plasmon resonance angle. The total angle shift gives the change in the effective optical thickness nd of the protein film, where n is the refractive index of the film and d is the thickness. Using the known thickness of the protein films, obtained from direct force measurements, we determined the protein surface coverage from the fitted index of refraction of the bound protein monolayer and a refractive index of 1.45 for the pure protein (Sivasankar et al., 2001). The protein densities per unit area for all cadherin segments studied are summarized in Table 1. The density of the different cadherin fragments bound to the immobilized SpA_{B2} monolayers is similar for all fragments, making the relative comparisons of the adhesive strengths between different fragments straightforward.

By precisely controlling the membrane distances D (Israelachvili, 1973) and hence the extent of overlap between opposed proteins, we established that FcCEC1-5 protein monolayers adhere at three distinct membrane separations (Fig. 2 A)—that is, at three different cadherin alignments. Upon approach, the two protein layers repelled at $D < 580$ Å. This is due to the steric repulsion between the end-on oriented ectodomains. When the surfaces were separated from distances $D < 370$ Å (Fig. 2 A, circles), where cadherins can interact along their entire lengths, the maximum adhesion was at $D = 382 \pm 6$ Å. This corresponds to binding between the fully interdigitated protein monolayers (Fig. 2 B). When the surfaces were separated from distances $390 \text{ Å} < D < 344 \text{ Å}$ (Fig. 2 A, triangles), which allows only partial cadherin overlap, the proteins adhered at $D = 445 \pm 10$ Å. If only the outermost domains overlapped at distances $460 \text{ Å} < D < 530 \text{ Å}$ (Fig. 2 A, squares), the adhesive minimum was again farther out at 531 ± 8 Å. The relative protein alignments that correspond with the distances of each of these minima are illustrated in Fig. 2 B. These results agree with measurements between His₆CEC1-5 monolayers (Sivasankar et al., 1999, 2001). However, between FcCEC1-5 monolayers, the three adhesive minima are shifted farther out by 120 ± 10 Å relative to those between His₆CEC1-5. The shift agrees quantitatively with the added lengths of the 45 Å Fc domains plus the measured 15 Å per immobilized protein A monolayer ($120 = 2 \times (45 + 15)$) (cf. Fig. 1). Importantly, this agreement with the previous findings (Sivasankar et al., 2001) confirms the specificity of these three homophilic cadherin binding interactions, which are independent of the cadherin construct or the anchoring method.

In all cases investigated in this study, there was no evidence of any damage to the membranes upon protein detachment. Measurements of the force profiles taken immediately

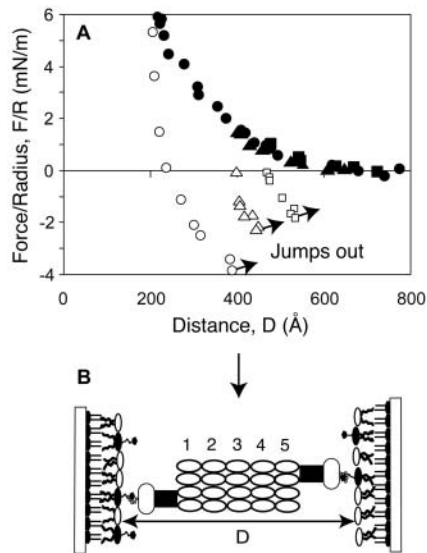


FIGURE 2 (A) Normalized force between oriented FcCEC1-5 monolayers versus the distance between the supporting membranes. CEC1-5 dimers fused with the Fc domain were immobilized on supported protein A monolayers. The cadherin density on each membrane was $9.9 \pm 0.4 \times 10^3$ cadherin/ μm^2 . The bathing medium contained 10 mM Tris buffer, 150 mM NaNO_3 , and 2 mM CaCl_2 at pH 7.0. The temperature was 25°C. Upon approach, the proteins repel at $D < 600$ Å. The filled circles indicate the forces measured during approach to $D < 400$ Å, and the open circles indicate forces measured during subsequent separation. At the position of the maximal attractive force, the protein-protein bonds yield and the surfaces jump out of adhesive contact. The filled and open triangles indicate the force curve measured during approach to $400 \text{ Å} < D < 500 \text{ Å}$ and separation, respectively. Squares show the force profile measured when the minimal separation was $D > 500$ Å. (B) Illustration of opposed, immobilized FcCEC1-5 monolayers.

after were identical to those taken before the pull-off. During surface detachment, the pull-out of the lipid anchors or the rupture of the protein-lipid linkage would irreversibly damage the protein monolayers, and thereby irreversibly alter subsequently measured force profiles (Leckband et al.,

1995). This absence of damage is expected, given the estimated cadherin bond energies (Table 2), which are lower than those shown previously to favor lipid extraction over bond rupture (Leckband et al., 1995).

Force measurements with five different domain deletion mutants (Table 1) identified the cadherin domains required for each of the three adhesive interactions. In previous flow assays, cells expressing the wild-type cadherin bound FcCEC1-5, FcCEC1-4, and FcCEC1-3 all similarly well (Chappuis-Flament et al., 2001). The direct force measurements described in this report elucidated the likely molecular mechanism responsible for the similarities. Fig. 3 A shows that FcCEC1-4 fragments also adhere in three antiparallel alignments, despite the loss of EC5. The first (inner), second (middle), and third (outer) minima occur at 297 ± 6 Å, 356 ± 2 Å, and 431 ± 9 Å, respectively (Table 2). The loss of EC5 in FcCEC1-4 shortens the protein by 43 ± 2 Å, and the positions of the three minima are correspondingly shifted inward by 85 ± 8 Å, in quantitative agreement with the loss of one domain from each cadherin (Fig. 3 B) (Table 2). The depths of the minima, at comparable protein surface densities and loading rates, are reduced by 40–50%, suggesting that the loss of EC5 impairs the overall adhesive activity without altering the binding mechanism—that is, without altering the number of adhesive alignments formed.

Similarly, FcCEC1-3 also adheres at the three membrane separations of 211 ± 9 , 269 ± 2 , and 349 ± 5 Å (Table 2). The average shifts in the positions of the three adhesive minima, relative to those between FcCEC1-4, are 83 ± 5 Å, consistent with the loss of a single domain from each protein. The positions of the minima differ from those of FcCEC1-5 by 176 ± 6 Å, or four times the length of a cadherin domain ($=4 \times \text{EC} = 172$ Å). In sharp contrast, FcCEC12 adheres extremely weakly at a single distance roughly commensurate with direct EC1/EC1 contact (Fig. 4). The latter weak adhesion agrees with cell adhesion and bead aggregation data (Chappuis-Flament et al., 2001). Importantly, the finding that EC1-3, EC1-4, and EC1-5 all bind in three

TABLE 2 Adhesion between cadherin ectodomain fragments

Cadherin fragment	1st minimum (inner)	F/R , mN/m (energy per bond, kT)*	2nd minimum (middle)	F/R , mN/m (energy per bond, kT)*	3rd minimum (outer)	F/R , mN/m (energy per bond, kT)*
CEC1-5 vs. CEC1-5	384 ± 6 Å	-3.6 ± 0.4 (19 kT)	445 ± 10 Å	-2.4 ± 0.5 (12 kT)	531 ± 6 Å	-1.8 ± 0.6 (9 kT)
CEC1-4 vs. CEC1-4	297 ± 6 Å	-1.4 ± 0.3 (6 kT)	356 ± 2 Å	-0.9 ± 0.2 (3.9 kT)	431 ± 2 Å	-0.22 ± 0.02 (0.9 kT)
CEC1-3 vs. CEC1-3	211 ± 9 Å	-1.2 ± 0.3 (4 kT)	269 ± 2 Å	-0.15 ± 0.01 (0.5 kT)	349 ± 5 Å	-0.17 ± 0.05 (0.6 kT)
CEC1-2 vs. CEC1-2	—	—	—	—	271 ± 14 Å	-0.3 ± 0.1 (0.9 kT)
CEC3-5 vs. CEC3-5	386 ± 4 Å	-0.5 ± 0.1 (2 kT)	—	—	—	—
CEC1245 vs. CEC1245	—	—	—	—	424 ± 8 Å	-0.7 ± 0.1 (3 kT)
CEC123 vs. CEC345	285 ± 9 Å	-0.5 ± 0.2 (2 kT)	—	—	—	—
CEC1245 vs. CEC345	—	—	—	—	—	—
CEC1-5 vs. CEC1245	—	—	—	—	493 ± 6 Å	-1.3 ± 0.2 (7 kT)
CEC1-5 vs. CEC345	375 ± 8 Å	-0.9 ± 0.2 (5 kT)	—	—	—	—

*The average bond energy is estimated from the protein surface density, the pull-off force F_{po} , and the Johnson Kendall Roberts theory of the adhesion between deformable solids (Johnson et al., 1971). The energy density per area between the two surfaces $E = 2F_{\text{po}}/3 \pi R$. The average bond energy E_b is then estimated by scaling the adhesion energy by the density of proteins on the surface Γ (cadherin/ Å^2), or $E_b = E/\Gamma$.

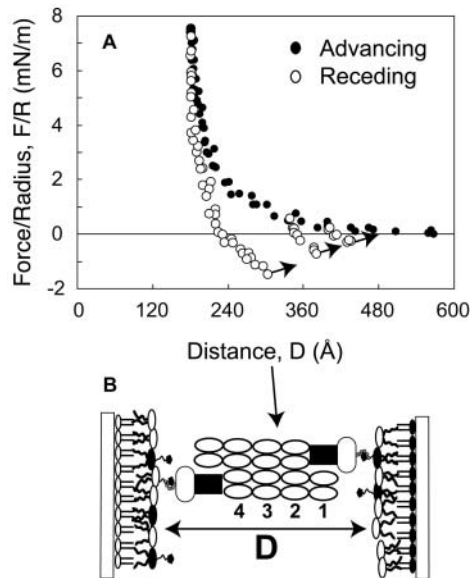


FIGURE 3 (A) Normalized force between oriented FcCEC1-4 monolayers versus the distance between the supporting membranes. The lipid monolayer composition was as described in Fig. 1, and the solution conditions are given in the text. This truncated cadherin fragment also adhered at three different antiparallel alignments. The positions of these three minima are shifted 120 Å relative to the three minima in Fig. 2. The FcCEC1-4 surface density was $1.2 \pm 0.4 \times 10^4$ cadherin/ μm^2 . (B) Illustration of the opposed, immobilized FcCEC1-4 monolayers.

distinct, antiparallel alignments, together with the quantized 85 ± 5 Å shifts in the positions of the adhesive minima upon removing successive domains, demonstrates that the adhesive mechanism is the same for all three mutants.

The location of the primary minimum between FcCEC1-3 fragments coincides with EC3/EC3 overlap, suggesting that EC3/EC3 adhesion generates the innermost minimum (cf. Fig. 2 A). This is confirmed by the finding that FcCEC3-5 fragments also bound each other, but at a single distance of 386 ± 5 Å (Fig. 5 A). The latter position corresponds to EC3/EC3 contact between the EC345 fragments (Fig. 5 B), and it is identical to the position of the primary minimum between FcCEC1-5 fragments (Table 2). CEC345 also bound CEC1-5 at 375 ± 8 Å, which is exactly the same distance as the first minimum measured between full-length CEC1-5. In addition, CEC345 bound CEC123 at 285 ± 9 Å, which is also the distance at which the EC3 domains would overlap. In all of these cases, which each involve interactions between different cadherin fragments, the positions of the minima are at distances of EC3/EC3 overlap (Table 2).

The role of EC3 was further confirmed by the adhesion between CEC1-5 and CEC345, which occurred at the single distance of 375 ± 8 Å. Again, this is identical to the location of both the first adhesive interaction between CEC1-5 monolayers and the homophilic adhesion between CEC345 fragments. Interestingly, the magnitude of the adhesion is approximately twice that measured either between identical EC345 fragments or between EC123 and EC345. This

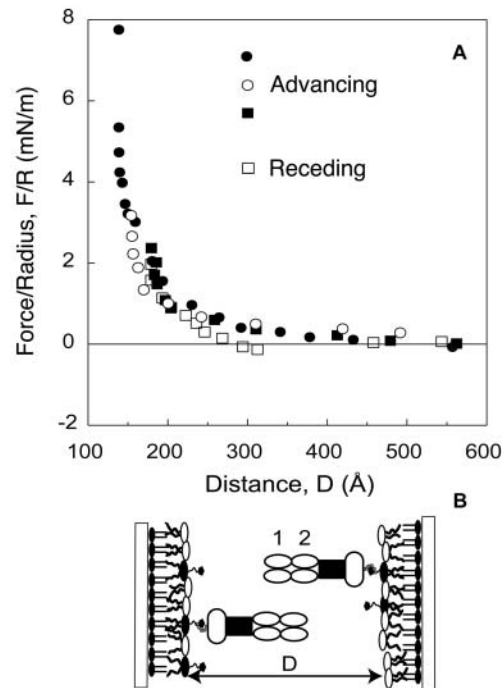


FIGURE 4 (A) Normalized force between oriented, immobilized FcCEC12 monolayers versus the distance between the supporting membranes. The lipid composition and solution conditions were as described in the text. The cadherin surface density was $1.7 \pm 0.4 \times 10^4$ cadherin/ μm^2 . These proteins adhered at a single, unique distance of 271 ± 14 Å. (B) Illustration of the corresponding immobilized FcCEC12 monolayers.

difference suggests that the other domains in the protein do have some influence on the function of EC3, and that their removal impairs EC3 activity. This hypothesis is supported by a recent study showing that cells expressing cadherin which lack EC1 do not adhere, but they do adhere to cells expressing the full-length EC1-5 (Renaud-Young and Gallin, 2002).

In contrast to the three adhesive bonds between antiparallel CEC1-5 monolayers, the full-length protein bound CEC1245 at a single distance of 493 ± 8 Å. This position differs by ~ 40 Å from that of the outer adhesive minimum between the full-length CEC1-5 proteins. Attributing the adhesion to the same interaction that forms the outer CEC1-5 bond, this is as expected since CEC1245 is shorter than CEC1-5 by a single domain. The absence of the first and second adhesive minima agrees with measurements between CEC1245 fragments and confirms the role of EC3 in the formation of those two adhesive bonds. Interestingly, the magnitude of the adhesion at -1.3 ± 0.2 mN/m is, within experimental error, comparable to the outer adhesive bond between identical CEC1-5 monolayers. At the same time, the adhesion is stronger than between identical CEC1245 domains. This further indicates that removing domains does have some impact on the function of the remaining segments.

This unexpected finding that EC3 also participates in

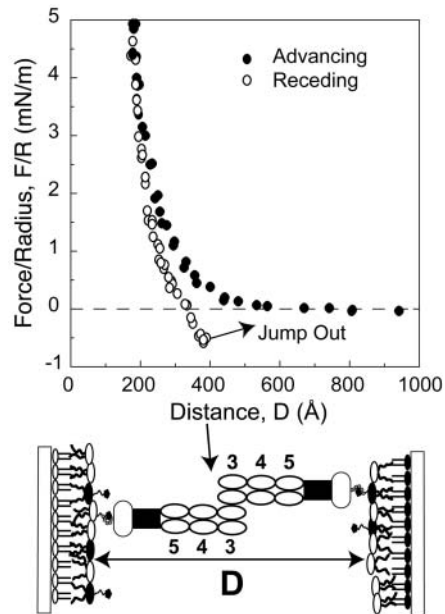


FIGURE 5 (A) Normalized force between oriented, immobilized FcCEC345 monolayers as a function of the distance between the supporting membranes. The lipid composition and solution conditions were as described in Fig. 1. The cadherin surface density was $1.2 \pm 0.4 \times 10^4$ cadherin/ μm^2 . This protein fragment undergoes homophilic adhesion at a single distance of 386 ± 4 Å. (B) Illustration of the corresponding immobilized FcCEC345 monolayers.

homophilic adhesion is based on direct measurements of cadherin's adhesive characteristics. Based on the range of protein binding relative to the protein dimensions, the strongest of the three bonds involves EC3/EC3 contact. This conclusion is based on the results of the many measurements described in this study, which include both homotypic and heterotypic interactions with several different fragments. The latter provide independent evidence for the participation of EC3 in homophilic cadherin adhesion. Moreover, these results explain the recent finding that E-cadherin mutants lacking EC1 still bind to the wild-type protein (Renaud-Young and Gallin, 2002).

Whereas the strongest adhesion occurred at EC3/EC3 overlap, the isolated EC345 fragments were poor adhesion proteins. In addition, EC345 did not reproducibly support cell attachment in flow assays, and mediated bead aggregation 30% of the time (Chappuis-Flament et al., 2001). The low EC345 adhesion could be due to structural changes due to the EC12 deletion. Despite efforts to avoid impairing protein function, structural changes often alter function in unanticipated and undesired ways. The difference in the adhesion between CEC345 and CEC1-5 versus CEC345 supports this idea, as does the reduced potency of increasingly shortened fragments. Alternatively, the EC345 fragment may require *cis* dimerization for full function, mediated either by EC1 or by the cytoplasmic domain, and thus requires interactions that are absent in EC345 (Yap et al., 1997a). Nevertheless, with EC1-3, EC1-4, and EC1-5, the

strongest bond always occurred at distances commensurate with direct EC3/EC3 contact, and removing this domain eliminated the strongest, inner homophilic bond.

With regard to the outermost bonds, the distances at which they form with CEC1-5, CEC1-4, CEC1245, CEC1-3, and CEC12 all correspond to distances of direct EC1/EC1 contact. We therefore attribute the outermost bond to homophilic adhesion between EC1 domains, in agreement with the proposed EC1 involvement in *trans* interactions (Pokutta et al., 1994; Shapiro et al., 1995; Ahrens et al., 2002; Boggon et al., 2002). Furthermore, homophilic CEC1245 binding occurred at a *single* distance of 424 ± 8 Å, which is identical to that of the outer bond between FcCEC1-4 fragments having identical length. Although this does not resolve the controversy over the true EC1-EC1 interface, these data do show that the outer domains adhere. The magnitudes of the adhesion between the outer domains that were measured with the different fragments do differ. This is attributed to the subtle effects of domain alterations, which could slightly affect the activity of the functional domains.

Importantly, we showed that the removal of EC1 abrogates not only the outer bond, but also the middle (second) bond. EC1 therefore participates in two binding interactions that each involve different domains. On the other hand, the removal of EC3 to yield CEC1245 abolished both the first and the second adhesive interactions. This suggests that the second (middle) bond may result from adhesion between EC3 and EC1 or from binding between EC1 and a site near the EC3/EC4 junction. The distance between the first and second minima measured with EC1-5, EC1-4, and EC1-3 is 59 ± 2 Å, which corresponds to a distance of ~ 1.5 domains. A bend in the structure between EC5 and EC3 (Boggon et al., 2002) would influence this distance, so that the bond may be due to EC1/EC3 contact. Other studies suggest that direct EC1/EC3 contact may not form the middle bond. EC345 did not bind EC1245, and EC345 did not bind EC123 at the distance of EC1/EC3 overlap. This argues against EC1/EC3 adhesion. However, because of the lack of domain reciprocity in the heterotypic fragment measurements, e.g., EC123 versus EC345, there is only half the number of potential EC1/EC3 contacts compared with interactions between identical fragments, e.g., EC123 versus EC123. Given the weak binding by EC345, EC123, and EC1245 (outer bond), reducing the number of reciprocal domain contacts could reduce the adhesion to below the detection limit. Alternatively, EC1 could bind the opposing protein near the EC3/EC4 junction. Nevertheless, although these measurements do not identify precise domain interface, the second minimum clearly requires both EC1 and EC3, directly implicating these *two domains* in the formation of the second (middle) bond.

We considered whether cadherin flexibility could underlie these results. However, this cannot account for the three minima for several reasons. First, there is no evidence for three discrete bends in either the protein or the ethylene oxide tether. EM images of cadherin ectodomains (Pokutta

et al., 1994) display a range of smoothly curved arcs with a variety of solid bend angles, and there is no evidence for three statistically distinct bend angles in the ectodomains. Second, x-ray reflectivity studies of cadherin monolayers show a flat electron density profile normal to the membrane with a smoothly decaying tail at the outermost edge (Martel et al., 2002). The profile does not exhibit three steps such as three discrete bend angles would generate. Third, the stiffness k of a rod decreases with the third power of the length: $k \propto L^{-3}$. If bond rupture occurred from different bent configurations, then shorter, stiffer fragments would not bend to the same extent under comparable loads, and the bonds would rupture at different apparent domain alignments. This is not observed. Along these lines, EC1245, which forms a *single* bond, lacks EC3 but should have the same flexibility as EC1234, which forms three bonds.

Direct measurements with the proteins CD2 and CD48 rule out anomalous tether bending (Zhu et al., 2002). We measured a single CD2-CD48 adhesive interaction at the exact distance predicted from the crystal structure (Zhu et al., 2002). The fragments EC1245, EC12, and EC345 also bound at unique distances. The NTA-lipid anchoring in all of these cases was identical.

There are differences in the measured homophilic adhesion between the mutants CEC1-5, CEC1-4, and CEC1-3 that were not evident, within experimental error, in the cell adhesion studies (Chappuis-Flament et al., 2001). This is most likely because the flow assays measured fragment adhesion against the full-length protein, rather than between identical fragments, as in this study. The force measurements that would be analogous to the flow assays would measure adhesion between FcCEC1-5 and the different fragments. The adhesion between CEC1-5 and either CEC1245 or CEC345 show that the deletion mutants indeed bind more strongly to the full-length protein than to themselves (Table 2). We similarly expect that stronger CEC1-3 and CEC1-4 adhesion to the full ectodomain would reduce apparent differences in the potency of these fragments. Differences in trends seen in flow assays versus the force measurements could also be due to difficulty in quantifying the absolute protein densities in the flow assays. Uncertainty in the protein densities as well as experimental error could mask subtle differences in fragment adhesion in the latter measurements.

It is important to comment on the results of these measurements of cadherin's adhesive properties in the context of existing structural data. Any of the models for *trans* interactions between N-terminal domains can account for the EC1/EC1 adhesion reported here. There are several reasons why we measure EC3/EC3 and putative EC1/EC3 contacts that were not seen in the crystal of the full ectodomain. In particular, contacts in crystal lattices represent the physiological ones, only if the physiological, molecular arrangement is compatible with the three dimensional, crystal lattice. This would not be the case if, for exam-

ple, cadherin arrangements at cell-cell junctions require both *cis* and *trans* contacts. If, because of symmetry, both contacts cannot coexist in the lattice, then the physiological complex will not crystallize, even though the protein obviously does. Additionally, packing constraints in crystals are nonphysiological, and packing forces can influence the structures formed, particularly when the specific bonds are weak. Conversely, membrane anchoring constrains proteins in ways that are absent in solution, i.e., by pinning. For these reasons, as well as others, interpretations of crystal structures are always tested against experimental measurements of protein function such as described here.

These new findings raise questions as to whether these three binding interactions occur between cells, and what the implications of such a binding mechanism could be. That EC3 participates in homophilic adhesion on the cell is supported by a report that cells displaying an EC1 deletion mutant still aggregated cells expressing the full length cadherin (Renaud-Young and Gallin, 2002). The possible implications of multiple bond formation were suggested by our previous demonstration that the successive rupture of these bonds could play a stabilizing role by impeding the adhesive failure of cadherin junctions (Sivasankar et al., 2001). Force measurements also suggested that sequential bond formation could facilitate junction assembly. If the outer domains were brought to contact, the protein monolayers slowly but *spontaneously* jumped into the more deeply interdigitated state, in the absence of any external force. This suggests a mechanism in which the outer domains control the initial recognition, but once cells adhere, the proteins slowly achieve the more stable, i.e., lower energy, interdigitated configuration. Understanding cadherin function may therefore require not only investigating cell aggregation but also quantifying the dynamics of adherens junction assembly and adhesion strengthening.

In summary, these direct quantitative adhesion measurements confirmed the specificity of the three adhesive interactions between full-length C-cadherin ectodomains, and identified the domains that are required for each of these three interactions. This leads to the model shown in Fig. 6 in which the outermost and innermost adhesive bonds are due to EC1/EC1 and EC3/EC3 adhesion, respectively, and the middle bond requires both EC1 and EC3. Importantly, techniques used to investigate protein function typically rely on measurements of single parameters or static structures and therefore cannot easily resolve mechanisms where protein function involves multiple domains capable of participating in multiple interactions. The distance resolution of these direct force measurements enabled us to show clearly and reproducibly with multiple, different fragments that two cadherin domains in fact participate in homophilic adhesion. The resultant domain interactions in turn give rise to a simple, modular binding mechanism in which cadherin ectodomains adhere in any of three antiparallel alignments. Previous dynamic force data suggested a potential role of this binding

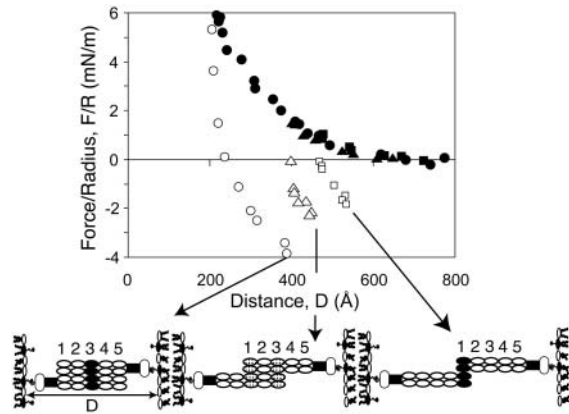


FIGURE 6 Model showing the domains required for the three adhesive minima between full-length cadherin ectodomains. The upper panel indicates the scaled energy-distance profile between FcCEC1-5 monolayers. The cartoons shown in Fig. 6 B indicate the domains required for each of the three adhesive interactions indicated in Fig. 6 A. The innermost adhesive minimum requires EC3 (black domains), the second minimum requires domains 1 and 3 (gray), and the outer minimum requires EC1 (black domains).

motif in stabilizing intercellular junctions (Sivasankar et al., 2001), but further studies will be needed to fully establish the biological implications of this binding mechanism and its role in cell adhesion selectivity.

We acknowledge Jonathan Goldberg, Mair Churchill, and William Weis for helpful discussions and comments regarding this work.

This work was supported by NIH R01 GM51338 (D.E.L.) and NIH R01 GM52717 (B.M.G.).

REFERENCES

- Ahrens, T., O. Pertz, D. Häussinger, C. Fauser, T. Schulthess, and J. Engel. 2002. Analysis of heterophilic and homophilic interactions of cadherins using the c-Jun/c-Fos dimerization domains. *J. Biol. Chem.* 277:19455–19460.
- Baumgartner, W., P. Hinterdorfer, W. Ness, A. Rash, D. Vestweber, H. Schindler, and D. Drenckhahn. 2000. Cadherin interaction probed by atomic force microscopy. *Proc. Natl. Acad. Sci. USA.* 97:4005–4010.
- Boggon, T., J. Murray, S. Chappuis-Flament, E. Wong, B. M. Gumbiner, and L. Shapiro. 2002. C-cadherin ectodomain structure and implications for cell adhesion mechanisms. *Science.* 296:1308–1313.
- Briehner, W. M., A. S. Yap, and B. M. Gumbiner. 1996. Lateral dimerization is required for the homophilic binding activity of C-cadherin. *J. Cell Biol.* 135:487–496.
- Chappuis-Flament, S., E. Wong, L. D. Hicks, C. M. Kay, and B. M. Gumbiner. 2001. Multiple cadherin extracellular repeats mediate homophilic binding and adhesion. *J. Cell Biol.* 154:231–243.
- Chothia, C., and E. Y. Jones. 1997. The molecular structure of cell adhesion molecules. *Annu. Rev. Biochem.* 66:823–862.
- Christenson, H., D. W. R. Gruen, R. G. Horn, and J. N. Israelachvili. 1987. Structuring in liquid alkanes between solid surfaces: Force measurements and mean field theory. *J. Chem. Phys.* 87:1834–1841.
- Davis, S. J., and P. A. van der Merwe. 1996. The structure and ligand interactions of CD2: implications for T-cell function. *Immunol. Today.* 17:177–187.
- Gumbiner, B. M. 1996. Cell adhesion: the molecular basis of tissue architecture and morphogenesis. *Cell.* 84:345–357.
- Häussinger, D., T. Ahrens, H.-J. Sass, O. Pertz, J. Engel, and S. Grzesiek. 2002. Calcium-dependent homoassociation of E-cadherin by NMR spectroscopy: changes in mobility, conformation, and mapping of contact regions. *J. Mol. Biol.* 324:823–839.
- Hunter, R. 1989. *Foundations of Colloid Science.* Oxford University Press, Oxford.
- Israelachvili, J. 1973. Thin film studies using multiple-beam interferometry. *J. Colloid Interface Sci.* 44:259–272.
- Israelachvili, J. 1987. Solvation forces and liquid structure, as probed by direct force measurements. *Acc. Chem. Res.* 20:415–421.
- Israelachvili, J. 1992a. Adhesion forces between surfaces in liquids and condensable vapours. *Surface Science Reports.* 14:110–159.
- Israelachvili, J. 1992b. *Intermolecular and Surface Forces.* Academic Press, New York.
- Israelachvili, J. N., and G. E. Adams. 1978. Measurement of forces between two mica surfaces in aqueous electrolyte solutions in the range 0–100 nm. *J. Chem. Soc. Faraday Trans. 1.* 75:975–1001.
- Israelachvili, J., and R. Pashley. 1983. Molecular layering of water at surfaces and origin of repulsive hydration forces. *Nature.* 306:249–250.
- Jensen, P., V. Soroka, N. K. Thompson, I. Ralets, V. Berezin, E. Bock, and F. M. Poulsen. 1999. Structure and interactions of NCAM modules 1 and 2, basic elements in neural cell adhesion. *Nat. Struct. Biol.* 6:486–493.
- Johnson, K. L., K. Kendall, and A. D. Roberts. 1971. Surface energy and the contact of elastic solids. *Proc. R. Soc. Lond. A.* 324:301–313.
- Kekicheff, P., W. A. Ducker, B. W. Ninham, and M. P. Pileni. 1990. Multilayer adsorption of cytochrome c on mica around isoelectric pH. *Langmuir.* 6:1704–1708.
- Kiselyov, V., V. Berezin, T. E. Maar, V. Soroka, K. Edvardsen, A. Schousboe, and E. Bock. 1997. The first immunoglobulin-like neural cell adhesion molecule (NACM) domain is involved in double-reciprocal interaction with the second immunoglobulin-like NCAM domain and in heparin binding. *J. Biol. Chem.* 272:10125–10134.
- Klingelhöfer, J., O. Y. Laur, R. B. Troyanovsky, and S. M. Troyanovsky. 2002. Dynamic interplay between adhesive and lateral E-cadherin dimers. *Mol. Cell Biol.* 22:7449–7458.
- Koch, A., D. Bozic, O. Pertz, and J. Engel. 1999. Homophilic adhesion by cadherins. *Curr. Opin. Struct. Biol.* 9:275–281.
- Lavrik, N., and D. Leckband. 2000. Optical and direct force measurements of the interaction between monolayers of aromatic macrocycles on surfactant monolayers. *Langmuir.* 16:1842–1851.
- Leckband, D. 2002. The structure of the C-cadherin ectodomain revealed. *Structure.* 10:739–740.
- Leckband, D., and J. Israelachvili. 2001. Intermolecular forces in biology. *Quart. Rev. Biophys.* 34:105–267.
- Leckband, D., W. Müller, F.-J. Schmitt, and H. Ringsdorf. 1995. Molecular mechanisms determining the strength of receptor-mediated intermembrane adhesion. *Biophys. J.* 69:1162–1169.
- Leckband, D., and S. Sivasankar. 2000. Mechanism of homophilic cadherin adhesion. *Curr. Opin. Cell Biol.* 12:587–592.
- Marra, J., and J. Israelachvili. 1985. Direct measurements of forces between phosphatidylcholine and phosphatidylethanolamine bilayers in aqueous electrolyte solutions. *Biochemistry.* 24:4608–4618.
- Martel, L., C. Johnson, S. Boutet, R. Al-Kurdi, O. Kononov, I. Robinson, D. Leckband, and J.-F. Legrand. 2002. X-ray reflectivity investigations of two-dimensional assemblies of C-cadherin: first steps in structural and functional studies. *J. Phys. IV.* 12:366–377.
- Nagar, B., M. Overduin, M. Ikura, and J. M. Rini. 1995. Structural basis of calcium-induced E-cadherin rigidification and dimerization. *Nature.* 380:360–364.

- Nose, A., K. Tsuji, and M. Takeichi. 1990. Localization of specificity determining sites in cadherin cell adhesion molecules. *Cell*. 61:147–155.
- Pertz, O., A. Bozic, W. Koch, C. Fauser, A. Brancaccio, and J. Engel. 1999. A new crystal structure, Ca^{2+} dependence and mutational analysis reveal molecular details of E-cadherin homoassociation. *EMBO J.* 18:1738–1747.
- Petrov, P., S. Miklavcic, U. Olsson, and H. Wennerstrom. 1995. A confined complex liquid. Oscillatory forces and lamellae formation from an L3 phase. *Langmuir*. 11:3928–3936.
- Pokutta, S., K. Herrenknecht, R. Kemler, and J. Engel. 1994. Conformational changes of the recombinant extracellular domain of E-cadherin upon calcium binding. *Eur. J. Biochem.* 223:1019–1026.
- Ranheim, T. S., G. M. Edelman, and B. A. Cunningham. 1996. Homophilic adhesion mediated by the neural cell adhesion molecule involves multiple immunoglobulin domains. *Proc. Natl. Acad. Sci. USA*. 93:4071–4075.
- Renaud-Young, M., and W. J. Gallin. 2002. E-cadherin EC1: heterophilic interactions, but not the conserved HAV motif, are required for adhesion. *J. Biol. Chem.* 277:39609–39616.
- Shan, W.-S., H. Tankaka, G. R. Phillips, K. Arndt, M. Yoshida, D. R. Colman, and L. Shapiro. 2000. Functional cis-heterodimers of N- and R-cadherins. *J. Cell Biol.* 148:579–590.
- Shapiro, L., A. M. Fannon, P. D. Kwong, A. Thompson, M. G. Lehmann, G. Grübel, J.-F. Legrand, J. Als-Nielsen, D. R. Colman, and W. A. Hendrickson. 1995. Structural basis of cell-cell adhesion of cadherins. *Nature*. 374:327–337.
- Sivasankar, S., W. Brieher, N. Lavrik, B. Gumbiner, and D. Leckband. 1999. Direct molecular force measurements of multiple adhesive interactions between cadherin ectodomains. *Proc. Natl. Acad. Sci. USA*. 96:11820–11824.
- Sivasankar, S., B. M. Gumbiner, and D. Leckband. 2001. Direct measurements of multiple adhesive alignments and unbinding trajectories between cadherin extracellular domains. *Biophys. J.* 80:1758–1768.
- Takeichi, M. 1991. Cadherin cell adhesion receptors as a morphogenetic regulator. *Science*. 251:1451–1455.
- Takeichi, M. 1995. Morphogenetic roles of classic cadherins. *Curr. Opin. Cell Biol.* 7:619–627.
- Tamura, K., W.-S. Shan, W. A. Hendrickson, D. R. Colman, and L. Shapiro. 1998. Structure-function analysis of cell adhesion by neural (N-) cadherin. *Neuron*. 20:1153–1163.
- Tomschy, A., C. Fauser, R. Landwehr, and J. Engel. 1996. Homophilic adhesion of E-cadherin occurs by a co-operative two-step interaction of N-terminal domains. *EMBO J.* 15:3507–3514.
- Vijayendran, R., D. Hammer, and D. Leckband. 1998. Simulations of the adhesion between molecularly bonded surfaces in direct force measurements. *J. Chem. Phys.* 108:1162–1169.
- Walsh, F., and P. Doherty. 1997. Neural cell adhesion molecules of the immunoglobulin superfamily. *Annu. Rev. Cell Biol.* 13:425–456.
- Wong, J. Y., T. L. Kuhl, J. N. Israelachvili, N. Mullah, and S. Zalipsky. 1997. Direct measurement of a tethered ligand-receptor interaction potential. *Science*. 275:820–822.
- Yap, A., W. M. Brieher, M. Ruschy, and B. M. Gumbiner. 1997a. Lateral clustering of the adhesive ectodomain: a fundamental determinant of cadherin function. *Curr. Biol.* 7:308–315.
- Yap, A. S., W. M. Brieher, and B. M. Gumbiner. 1997b. Molecular and functional analysis of cadherin-based adherens junctions. *Annu. Rev. Cell Dev. Biol.* 13:119–146.
- Yap, A. S., C. M. Niessen, and B. M. Gumbiner. 1998. The juxtamembrane region of the cadherin cytoplasmic tail supports lateral clustering, adhesive strengthening and interaction with p120ctn. *J. Cell Biol.* 141:779–789.
- Zhu, B., E. A. Davies, P. A. van der Merwe, T. Calvert, and D. E. Leckband. 2002. Direct measurements of heterotypic adhesion between the cell surface proteins CD2 and CD48. *Biochemistry*. 42:12163–12170.